Journal of Molecular Structure 1242 (2021) 130737

Contents lists available at ScienceDirect

Journal of Molecular Structure

journal homepage: www.elsevier.com/locate/molstr

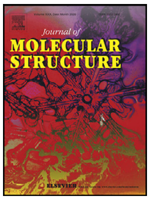

Terpyridine Zn(II) azide compounds: Spectroscopic and DFT calculations

Ahmed M. Mansour

Department of Chemistry, Faculty of Science, Cairo University, Gamma Street, Giza, 12613, Egypt

ARTICLE INFO

Article history:
Received 18 April 2021
Revised 17 May 2021
Accepted 18 May 2021
Available online 23 May 2021

Keywords:
Terpyridine
Zn(II) azide complexes
Vibrational analysis
TDDFT

ABSTRACT

Square-pyramidal Zn(II) azide complexes with the formula of $[Zn_n(N_3)_{2n}L]$ (n = 1; L = 4′-(2-pyridyl)-2,2′:6′,2′′-terpyridine (L^{Py}), 4′-(4-phenylmorpholine)-2,2′:6′,2′′-terpyridine (L^{Morph}), and n = 2; L = 1,4-*bis*(2,2′:6′,2′′-terpyridin-4′-yl)benzene (L^{BPY})) were synthesized, and structurally characterized using different spectroscopic and analytical tools. Ground-state geometry optimization and harmonic vibrational analysis were carried out at two different levels of theory (B3LYP/LANL2DZ and CAM-B3LYP/def2-SVP) to gather insights into the local minimum structures. Natural bond orbital (NBO) analyses revealed that the electronic population of the 3d orbitals of Zn(II) ion is corresponding to the oxidation state of Zn(I), not Zn(II), in agreement with the ligand to metal charge transfer. Molecular electrostatic potential energy maps showed that the azido ligand may act as a nucleophile in the cycloaddition coupling with electron poor dipolar molecules. The electronic structure and transitions were investigated by executing time dependent density functional theory (TDDFT) calculations.

1. Introduction

Zinc(II) ion, the second most plentiful d-block metal ion in the human body, is mostly static as cofactor for over 300 enzymes including anhydrases, aminopeptidases, alkaline phosphatases, etc., which participates in several metabolic processes of the living systems [1]. The function of aminopeptidases, a bridged binuclear Zn(II) complex, is the elimination of amino acids from the termini of the proteins and peptides. Alkaline phosphatase, phospholipase C, and nuclease P1 catalyse the hydrolysis of phosphoesters.

Benefiting from various coordination numbers, geometries, and exciting optoelectronic properties, coordination compounds of Zn(II) ion were widely investigated as catalysts [2], light-emitting diodes [3], and sensors [4,5]. For example, a fluorescent selective Zn(II) probe for thymine-rich single-stranded DNA over other DNA strains was fabricated from 1,4,7,10-tetraazacyclo-dodecane [5]. The coordination chemistry of Zn(II) with 2,2′:6′,2′′-terpyridine (terpy) is rich, and a subject of interest because of their exciting photophysical [6], and catalytic properties [7]. Among the complexes of $[M(L^{Py})_2](NO_3)_2$ (M = Co(II), Cu(II) and Zn(II)), Zn(II) complex exhibited a highly selective affinity to Fe(II) in the μM range over the other tested metal complexes [8]. A simple method for the optical discrimination of mercapto-based amino acids was established by using Zn(II) complex of 2-furyl-terpyridine, and corresponding amino acid [9]. Glassy carbon electrode decorated with Co(II) complex of 4′-phenyl-terpyridine showed good electrocatalytic performance during the reduction of hydronium ions into hydrogen [10]. Coordination of 4′-(4-(diphenyl-amino)thienyl)-2,2′:6′,2′′-terpyridine to Zn(II) improved significantly the nonlinear optical response in the near IR region [6]. The luminochromism behavior of Zn(II) terpyridine complex, decorated with triphenylamino group, induced by reversible ligand dissociation process, was reported [11]. Zn(II) complexes of 4′-phenyl-terpyridine (X = CH_3COO^-, Cl^-, NO_3^-, and SO_4^{2-}) exhibited promising *in vitro* antitumor activity against several malignant cells [12].

The selective chemical modification of biomolecules by the attachment of metal-based compound drives a significant piece of modern drug development. Owing to their high selectivity, click chemistry defines the extremely specific bio-orthogonal reactions [13] that are simple to execute with easily accessible chemicals. Selective labelling of biological molecules is one of the important applications of click reaction, which is essential to follow up the temporal feature of the biomolecule localization and its role within the cell. The [3+2] azide-alkyne cycloaddition reaction usually gives rise to a mixture of 1,4- and 1,5-disubstituted 1,2,3-triazoles [14], where the reaction kinetics, and the selectivity toward the formation of 1,4-isomer are enhanced by addition of Cu(I) ion [15], and regioselectivity to 1,5-isomer by using Ru(II) complexes [16].

Based on the well-known biological and industrial applications of Zn(II) complexes and the interest of our research group in the [3+2] cycloaddition coupling of azido metal complexes

---

E-mail address: mansour@sci.cu.edu.eg

https://doi.org/10.1016/j.molstruc.2021.130737
0022-2860/

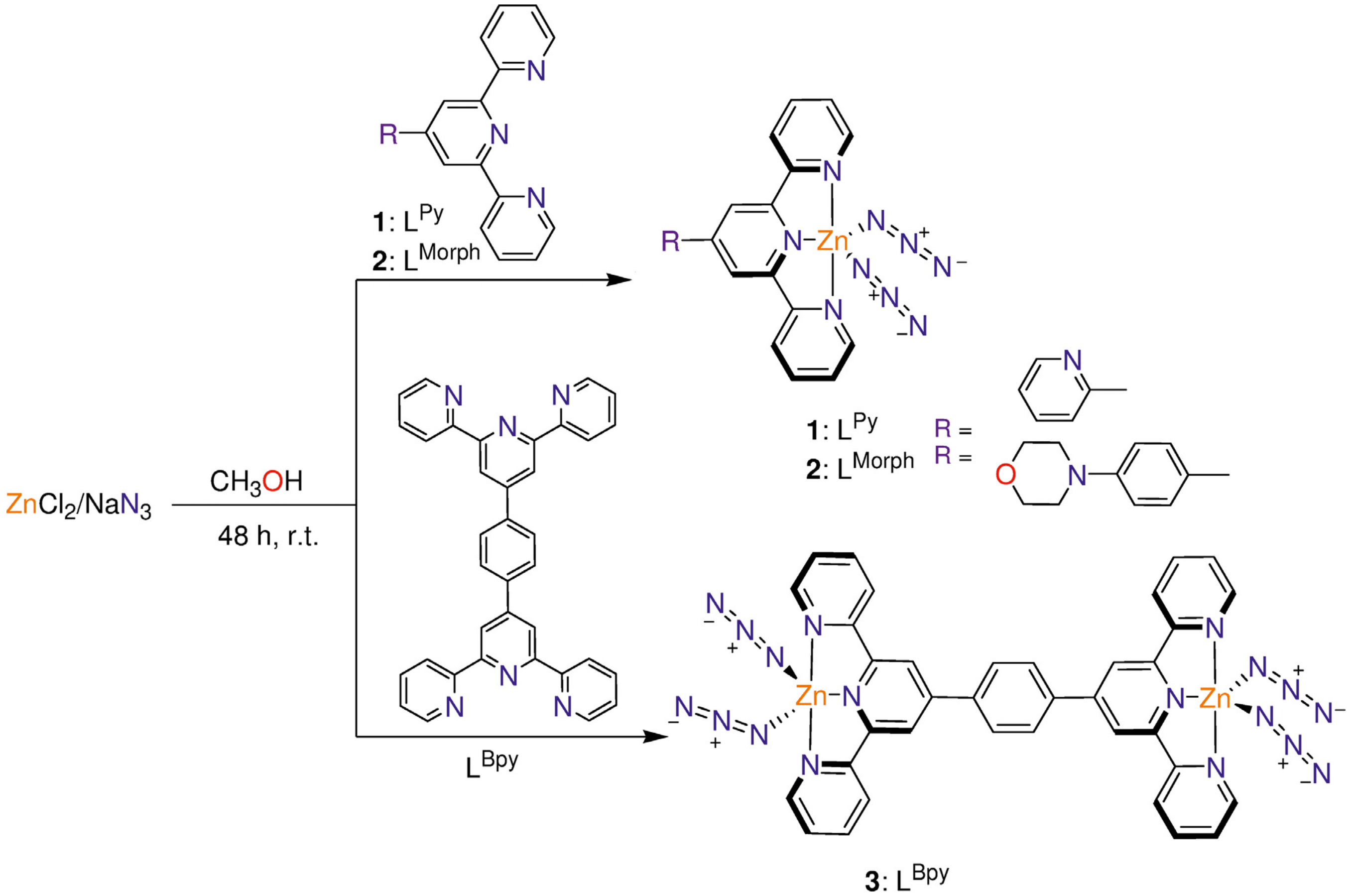

Scheme 1. Synthesis of terpyridine based Zn(II) azide complexes **1–3**.

[17–23], we became interested in synthesis, and characterization of mono-, and binuclear terpyridine based Zn(II) azide complexes (Scheme 1), to further investigate them in the catalyst-free [3+2] cycloaddition reaction under mild conditions. In addition to the spectroscopic analysis, density functional theory calculations were executed to gain some information about the molecular structures, vibrational, and electronic properties of the azide compounds.

2. Experimental section

2.1. Materials and instruments

The ligands; 4′-(2-pyridyl)-2,2′:6′,2′′-terpyridine (L^{Py}) [24], 4′-(4-phenyl morpholine)-2,2′:6′,2′′-terpyridine (L^{Morph}) [20] and 1,4-*bis*(2,2′:6′,2′′-terpyridin-4′yl)benzene (L^{BPY}) [20] were prepared in a pure form and good yield according to the published procedures. NMR analysis {^{1}H, and ^{13}C{^{1}H}} as well as two dimensional ({^{1}H, ^{1}H} COS90 and {^{1}H, ^{13}C} HSQC) were conducted using Bruker-Avance 400 spectrometer at the corresponding magnetic field. Solid-state IR analysis was executed on Nicolet 380 FT-IR spectrometer equipped with a smart iFTR accessory. Electrospray mass spectra were recorded on ThermoFisher Exactive Plus instrument with an Orbitrap mass analyzer at a resolution of R = 70.000 and a solvent flow rate of 50 µL min^{-1}. Elemental microanalysis was performed with a Vario Micro Cube analyzer of Elementar Analysensysteme or an EA 3000 elemental analyzer from HEKtech. Electronic absorption spectra of **1–3** were recorded on a Specord 210 Plus spectrophotometer.

2.2. Synthesis of azide complexes 1–3

2.2.1. Caution

Azide compounds are subjected to unexpected violent because of scratching, and hence handling and purification with great care are vital.

A mixture of terpyridine ligand [0.5 mmol; 155 mg (L^{Py}), 198 mg (L^{Morph}) and 270 mg (L^{BPY})], $ZnCl_2$ [0.5 mmol; 68 mg (L^{Py} and L^{Morph}) and 136 mg (L^{BPy})] and sodium azide [1.0 mmol, 65 mg (L^{Py} and L^{Morph}), and 2.0 mmol, 130 mg (L^{BPY})] was dissolved in CH_3OH and the reaction mixtures were stirred at the room temperature for 48 h. Precipitation occurred and the products were washed with methanol (3 × 5 mL), diethyl ether (2 × 5 mL) and then dried under vacuum over few days.

[Zn(N$_3$)$_2$L^{Py}] (**1**): White powder, yield: 83% (190 mg, 0.41 mmol). IR (ATR, diamond): ν = 3065 (w, CH), 2059 (vs, N_3), 1598 (s, CC/CN), 1471, 1437, 1410, 1158, 1014, 777, 725 cm^{-1}. ^{1}H NMR (DMSO-d$_6$, 400.40 MHz): δ = 9.28 (s, 2H), 8.90–8.81 (m, 3H), 8.81–8.68 (m, 2H), 8.58–8.48 (m, 1H), 8.37–8.22 (m, 2H), 8.09 (td, $J_{H,H}$ = 7.7 Hz, $J_{H,H}$ = 1.8 Hz, 1H), 7.94–7.77 (m, 2H), 7.63–7.58 (m, 1H) ppm. ^{13}C NMR (DMSO-d$_6$, 100.68 MHz): δ = 152.6, 151.5, 150.1, 149.2, 148.8, 147.0, 140.8, 137.8, 127.3, 125.6, 122.7, 119.7 (2C) ppm. ESI-MS (positive mode, methanol): m/z = 463.0742 {[Zn(N$_3$)$_2$L^{Py}]+H}$^+$, 419.0475 {[Zn(N$_3$)L^{Py}]}$^+$. $C_{20}H_{14}N_{10}Zn$: C 52.25, H 3.07, N 30.46, found C 52.57, H 3.11, N 30.08.

[Zn(N$_3$)$_2$L^{Morph}] (**2**): Yellow powder, yield 85% (233 mg, 0.43 mmol). IR (ATR, diamond): ν = 2056 (vs, N_3), 1591 (s, CC/CN), 1232, 791 cm^{-1}. ^{1}H NMR (DMSO-d$_6$, 400.40 MHz): δ = 8.98–8.81 (m, 4H), 8.81–8.66 (m, 2H), 8.27 (t, $J_{H,H}$ = 8.6 Hz, 2H), 8.16 (d, $J_{H,H}$ = 8.1 Hz, 2H), 7.90–7.77 (m, 2H), 7.07 (d, $J_{H,H}$ =

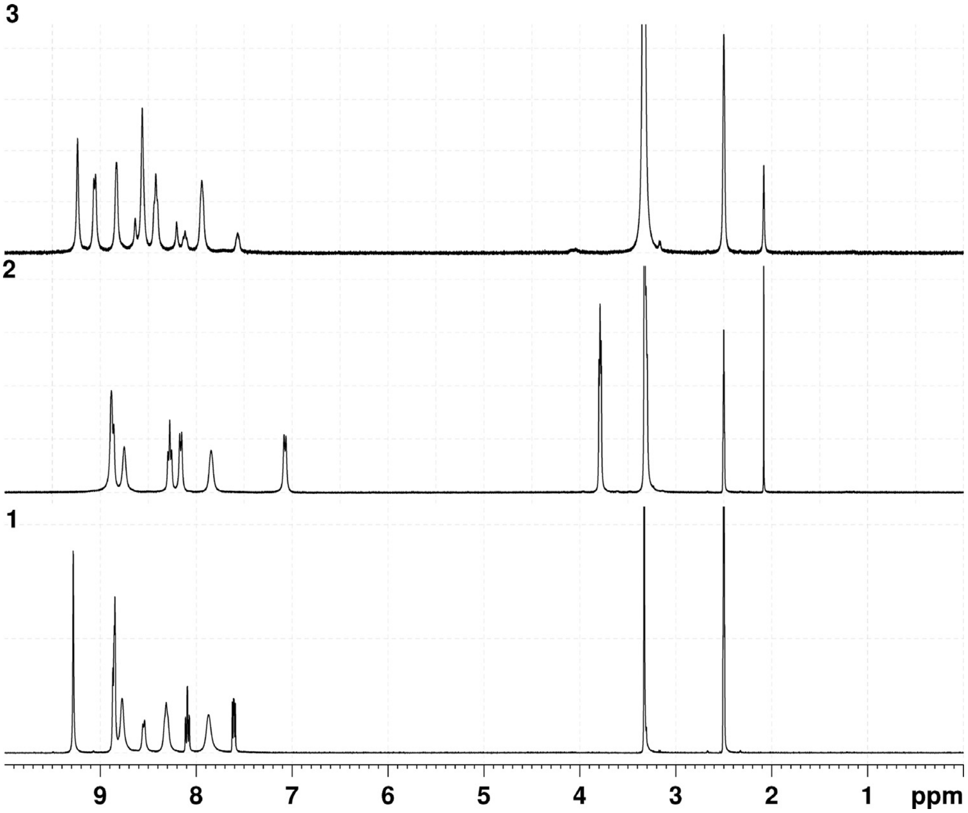

Fig. 1. ^{1}H NMR spectra of complexes **1–3** in DMSO-d$_6$. (The original spectra including the integrations are given in ESI file).

8.3 Hz, $J_{H,H}$ = 1.8 Hz, 2H), 3.82–3.74 (m, 4H, morpholine), 3.31–3.25 (m, 4H, morpholine) ppm. ^{13}C NMR (DMSO-d$_6$, 100.68 MHz): δ = 153.6, 152.8, 148.6, 147.5, 140.6, 128.9 (2C), 127.0, 122.6 (2C), 118.1, 114.2, 65.9 (morpholine-C), 47.1 (morpholine-C) ppm. ESI-MS (positive mode, methanol): m/z = 500.1171 {[Zn(N$_3$)L^{Morph}]}. $C_{25}H_{22}N_{10}OZn{\bullet}0.5H_2O$: C 54.31, H 4.19, N 25.33, found C 54.57, H 4.57, N 24.95.

[Zn$_2$(N$_3$)$_4$L^{BPy}] (**3**): Creamy white powder, yield: 73% (317 mg, 0.37 mmol). IR (ATR, diamond): ν = 2057 (vs, N$_3$), 1600 (s, CC/CN), 1475, 1015, 792 cm^{-1}. ^{1}H NMR (DMSO-d$_6$, 500.13 MHz): δ = 9.32–9.13 (m, 4H), 9.13–8.95 (m, 4H), 8.91–8.71 (m, 4H), 8.59–8.54 (m, 4H), 8.48–8.33 (m, 4H), 8.01–7.81 (m, 4H) ppm. ^{13}C NMR (DMSO-d$_6$, 100.68 MHz): δ = 153.2, 149.0, 148.8, 147.3, 140.9, 137.5, 128.9, 127.4, 123.2, 120.6 ppm. ESI-MS (positive mode, methanol): m/z = 757.4547 {[Zn$_2$(N$_3$)$_2$L^{BPy}]}$^{2+}$. $C_{36}H_{24}N_{18}Zn_2{\bullet}4H_2O$: C 47.43, H 3.54, N 27.66, found C 47.51, H 3.13, N 27.46.

2.3. Density functional theory calculations

Ground-state geometry optimization, and vibrational analysis of the azide compounds were performed by B3LYP/LANL2DZ and CAM-B3LYP/def2-SVP methods using Guassian03 [25]. Time-dependent density functional theory (TDDFT) calculations were executed at B3LYP/LANL2DZ level of theory using the polarizable continuum solvation model (PCM). Visualization of local minimum structures, vibrational IR, frontier molecular orbitals and molecular electrostatic potential energy maps were done using Gaussview03 **[**26**]**.

3. Results and discussion

3.1. Synthesis, and characterization

The functionalized terpyridine ligands; 4′-(2-pyridyl)-2,2′:6′,2′′-terpyridine (L^{Py}), 4′-(4-phenylmorpholine)-2,2′:6′,2′′-terpyridine (L^{Morph}) [24]**,** and 1,4-*bis*(2,2′:6′,2′′-terpyridin-4′-yl)benzene (L^{BPY}) [20] were prepared in one step *via* the reaction of 2-acetylpyridine with 2-pyridinecarboxaldehyde, 4-(4-morpholinyl)benzaldehyde, and terephthalaldehyde, respectively, in a strongly basic media. As shown in Scheme 1, Zn(II) azide complexes were prepared by stirring a mixture of the terpyridine ligand, zinc(II) chloride, and sodium azide in methanol for 48 h. The mono-, and binuclear zinc(II) complexes of the type [Zn$_n$(N$_3$)$_{2n}$L] (n = 1; L = L^{Py} (**1**) [27] & L^{Morph} (**2**), and n = 2; L = L^{BPY} (**3**)) were analytically and spectroscopically characterized using IR (Fig. S1), NMR (^{1}H, ^{13}C{^{1}H}, {^{1}H, ^{1}H} COS90 and {^{1}H, ^{13}C} HSQC)) (Fig. S2–S4), ESI MS(+), and elemental analysis. The IR spectra of the azide compounds **1**–**3** (Fig. S1) show the prominent azide stretching mode at 2059, 2055, and 2057 cm^{-1}. The ^{1}H, (Fig. 1) and ^{13}C NMR patterns of **1**–**3** confirm that the terpyridine ligands are in k^3-N^1,N^2,N^3 tridentate coordination mode. An additional evidence for the proposed azide structures was provided by positive mode ESI MS analysis, in which peaks corresponding to {[Zn(N$_3$)$_2$L^{Py}]+H}$^+$ (*m/z* = 463.0742), and {[Zn(N$_3$)L^{Py}]}$^+$ (*m/z* = 419.0475) are observed in the mass spectrum of **1**. For complex **2**, the mono azide fragment is detected at *m/z* = 500.1171. In the case of **3**, a characteristic peak is observed at *m/z* = 757.4547 matching the {[Zn$_2$(N$_3$)$_2$L^{BPY}]}$^{2+}$ fragment.

3.2. Density functional theory calculations

To get an insight into the geometrical, vibrational, and electronic structures of the azide Zn(II) complexes, ground-state geometry optimizations of models representing their molecular structures were done at two different levels of theories; B3LYP [28]/LANL2DZ [29] and CAM-B3LYP [30]/def2-SVP [31]. The atomic coordinates of the local minimum structures of **1**–**3** are given in Tables S1–5 and their corrected energies values are given in Table S6**.** The calculated Zn–N bonds, and N–Zn–N bond angles of

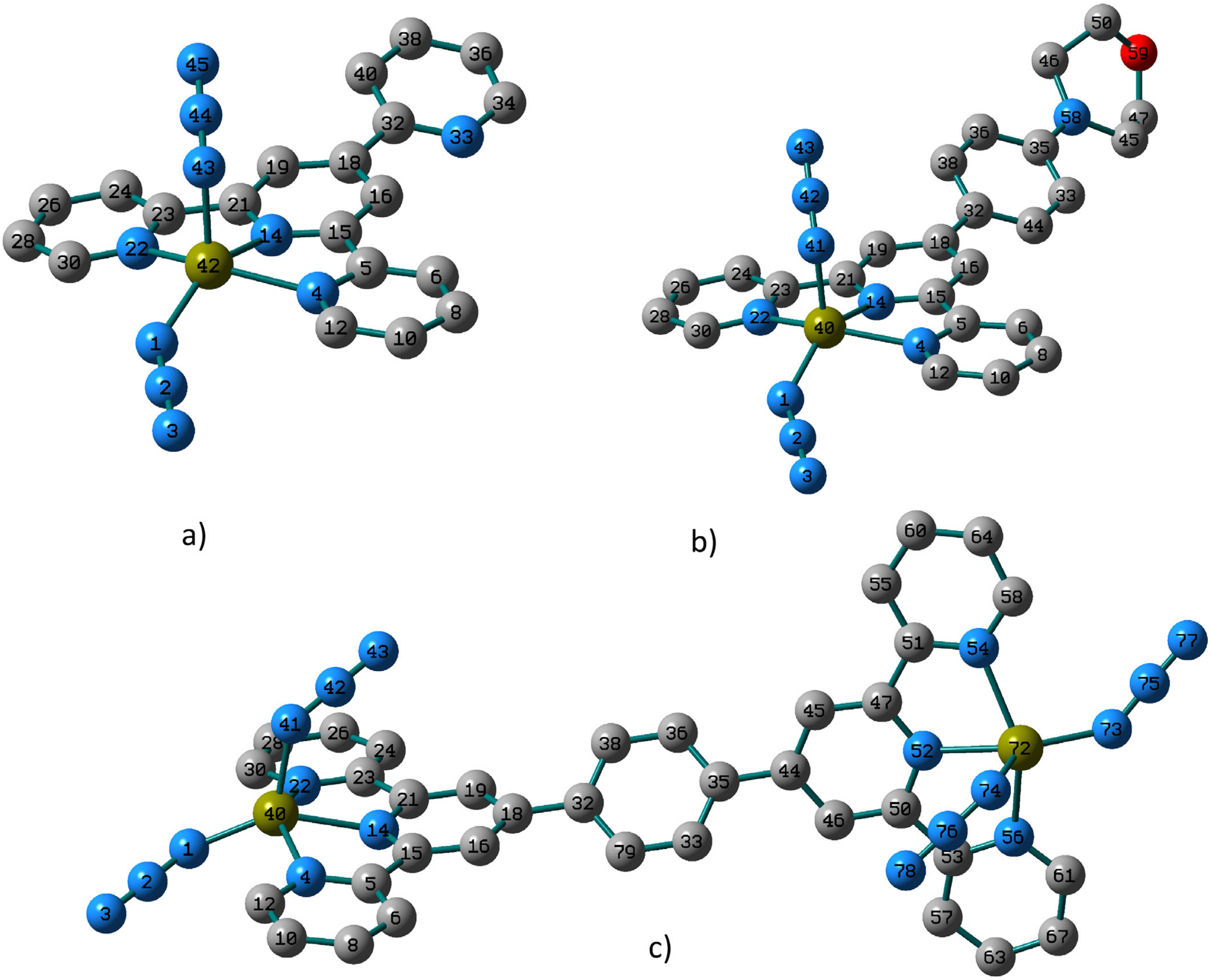

Fig. 2. Local minimum structures of the optimized azide Zn(II) complexes a) **1**, b) **2** and c) **3**, calculated at B3LYP/LANL2DZ level of theory. (H-atoms were omitted for the clarity).

1–**3** were tabulated together with the crystal data of compound **1** (Table S7) [27]. In general, the calculated bond lengths, and bond angles around Zn(II) ion in **1**–**3** are nearly the same, and does not alter by changing the type of the substituent. The optimized parameters of the two Zn(II) moieties of **3** are typical. Compared to the crystal data of **1**, the root mean square errors of the selected bond lengths are 0.05, and 0.27 Å for B3LYP/LANL2DZ and CAM-B3LYP/def2-SVP, respectively, indicating that B3LYP/LANL2DZ method is an appropriate calculation method for this size of metal-based compounds.

As shown in Fig. 2, the Zn(II) ion is five-coordinated by tridentate terpyridine ligand [Zn–N4 = 2.245 Å, Zn–N14 = 2.169 Å and Zn–N22 = 2.129 Å] and two azido ligands [Zn–N1 = 1.990 Å, and Zn–N43 = 2.042 Å], at B3LYP/LANL2DZ level of theory. For penta-coordinated Zn(II) complexes, the angular structural index parameter ($\tau = ((\alpha - \beta))/60$) could be used as an index to get an insight into the geometry of the complex in which $\tau = 0$ for a perfect square pyramidal, and $\tau = 1$ for a perfect trigonal-bipyramidal geometry (α and β are the two largest bond angles around the Zn(II) ion) [32]. The geometry around Zn(II) ion in **1–3** is best described as a perfect square-pyramidal ($\tau = 0$) in which the axial position is occupied by azide ligand, and the square-base by tridentate terpyridine ligand and another azide ligand. Similar to the crystal structure of **1**, the terminal azide ligands of the optimized structures are nearly linear [N1–N2–N3 = 178.0°, and N43–N44–N45 = 180.0°] and bond to Zn(II) ion with angles of 137.1° (Zn–N1–N2), and 125.2° (Zn–N43–N44). The terpyridine system is coplanar with the Zn(II) ion [N4–C5–C15–N14 = 6.4°, and N22–C23–C21–N14 = 4.3°]. For **1** and **2**, the pyridyl and morpholinyl rings are rotated out the plane by 16.4°, and 11.9° as defined by the dihedral angles of C16–C18–C32–N33, and C33–C35–N58–N45, respectively.

The obtained geometries were characterized as local minima because of the absence of the imaginary vibrational modes. The calculated vibrational spectra (Fig. S5) of **1**–**3** were executed by B3LYP/LANL2DZ, and CAM-B3LYP/def2-SVP methods. In general, the theoretical wavenumbers are expected to be higher than the experimental finding because of the basis set truncation, and the neglection of the electron correlation and mechanical anharmonicity especially in the range of the bending modes [33]. To compensate these limitations, the scaling methods should be introduced. The IR calculations give rise to two $\nu(N_3)$ values for the axial (2024–2041 cm^{-1}) and the equatorial azide ligands (2064–2067 cm^{-1}) (Fig. 3). The stretching mode of the axial azide ligand is shown as a shoulder in the experimental spectra. B3LYP/LANL2DZ

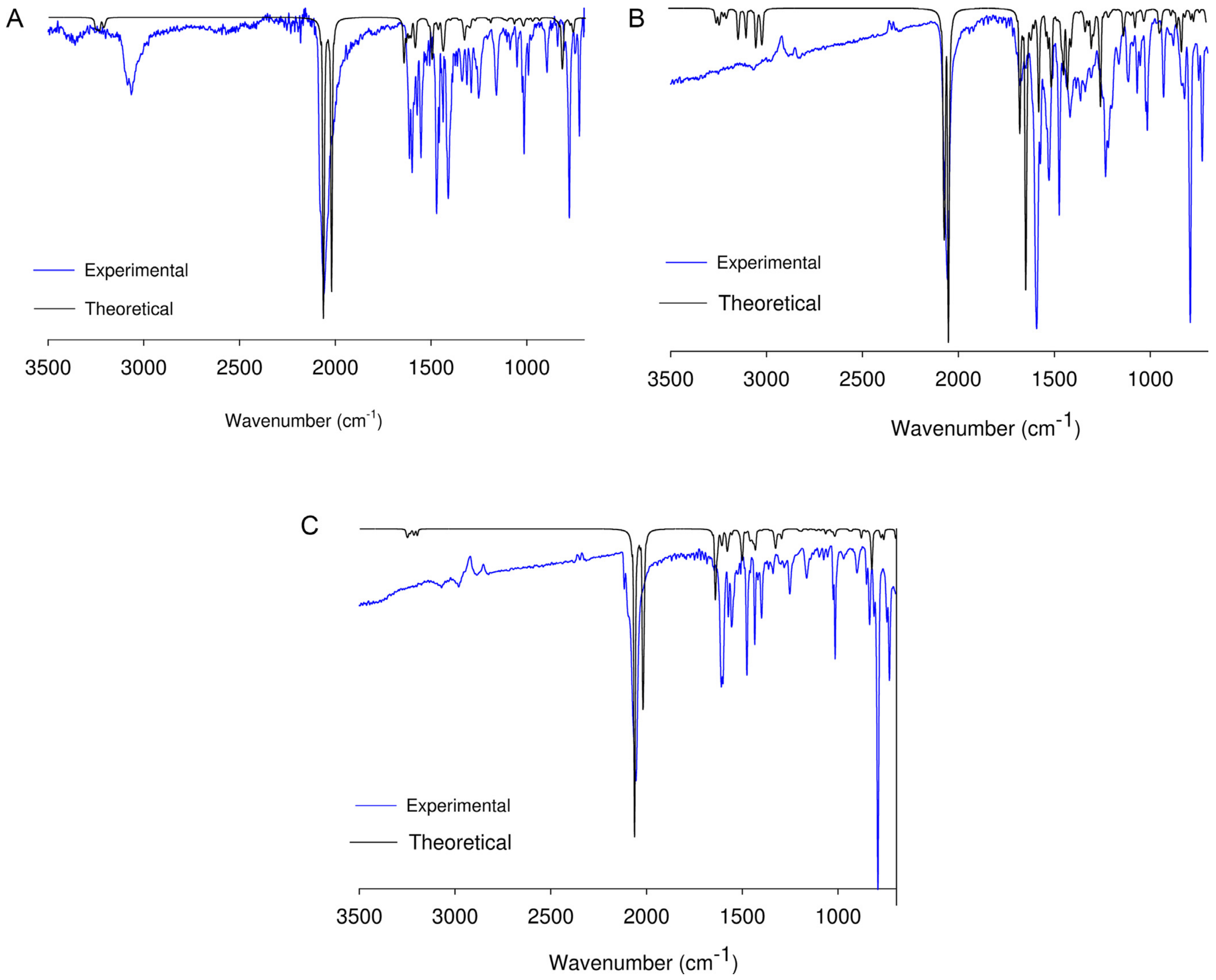

Fig. 3. Combined experimental and theoretical vibrational spectra of a) **1**, b) **2** and c) **3** calculated at B3LYP/LANL2DZ level of theory.

gives comparable results to the experimental finding, while a discrepancy of 100–150 cm^{-1} is recognized for the unscaled IR active modes, which were calculated by CAM-B3LYP/def2-SVP. Therefore, B3LYP/LANL2DZ method gives also better expectation for the wavenumbers of the azide stretching bands without the introduction of a scaling factor than B3LYP/def2-SVP method.

3.3. Natural bond orbital analysis

The natural bond orbital (NBO) analysis of Weinhold and coworkers [34] was executed for the local minimum structures of the Zn(II) azide complexes to gather insights into the natural charge of the metal ion, as well as the nature, strength and type of the hybridization of the bonds of the coordination sphere around Zn(II) ion. NBO analysis and second order perturbation theory analysis of Fock Matrix in NBO Basis were carried out by B3LYP/LANL2DZ method. The electronic configuration of Zn ion in **1** is [Ar]4s$^{0.30}$3d$^{9.97}$4p$^{0.44}$, the natural charge is 1.28719e and the residence of the 3d-subshell is as follows: $d_{xy}{}^{1.99492}d_{xz}{}^{1.99398}d_{yz}{}^{1.99609}d_{x2-y2}{}^{1.99600}d_{z2}{}^{1.99142}$. The 3d-electronic population of Zn ion is corresponding to the oxidation state of Zn(I), not Zn(II), in agreement with the ligand to metal charge transfer. The σ(Zn–N43) bond is created from sp$^{1.32}$d$^{0.02}$ hybrid on Zn atom (a mixture of 42.66% s, 56.49% p and 0.85% d) and sp$^{99.99}$ hybrid on N atom of the axial azide group (a mixture of 0.26% s, and 99.74% p) and is polarized towards N_3 group (95.42 %). The strength of the interactions between Zn(II) and ligands (terpyridine derivative and azide) could be deduced from E^2 values (the second order interaction energy between donor–acceptor orbitals in the complexes). The E^2 values are 1.38, 1.76, 11.63, 12.56, and 52.16 kcal mol^{-1} for LP(2)N1→, LP(1)N4→, LP(1)N14→, LP(1)N22→, and LP(1)N43→σ*(Zn–N43), respectively, reflecting that the terpyridine coordination nitrogen centres have different strengths of interaction with Zn(II) ion. Similar NBOs and second order interaction energy values are observed for compounds **2** and **3** excluding the role of the terpyridine substituent or the presence of two metal ions per compound in determining the nature of the NBOs.

3.4. Molecular electrostatic potential energy maps

Molecular electrostatic potential map is a suitable descriptor to discover the sites for H-bond interactions as well as electrophilic and nucleophilic attack [35]. The electrostatic potential values were calculated by B3LYP/LANL2DZ method and characterized by two different colours (Fig. 4); blue and red represent areas of the positive and negative electrostatic potential, respectively. For **1**–**3**, red regions are observed mainly over the coordination sphere includ-

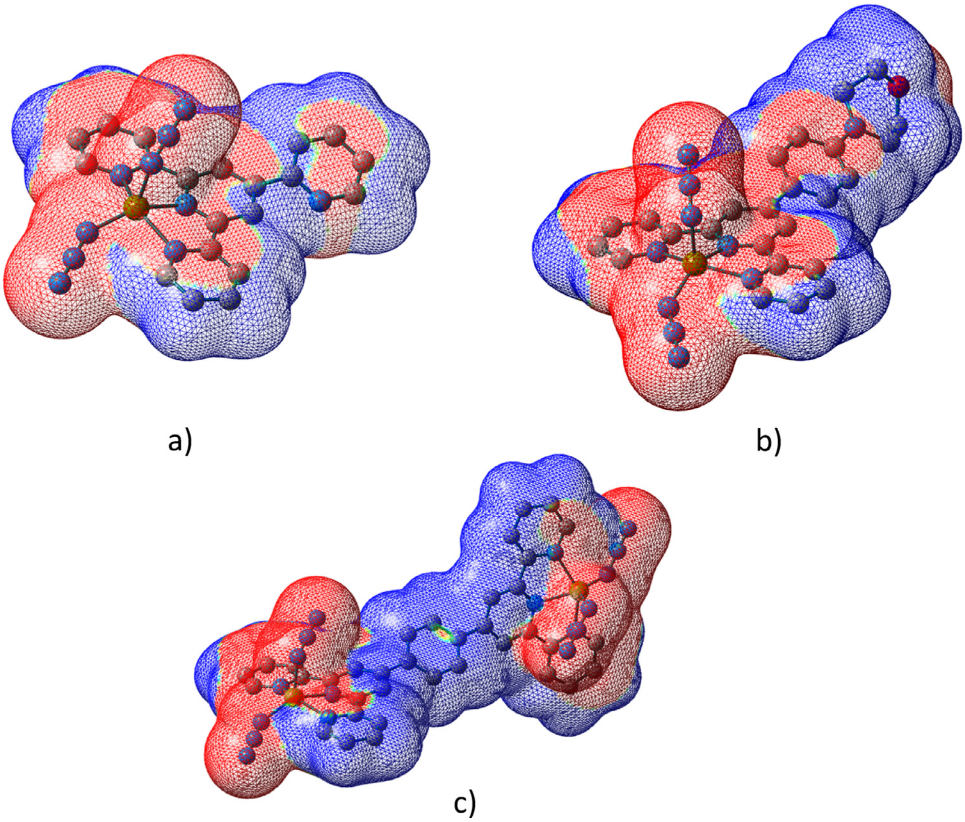

Fig. 4. Molecular electrostatic potential maps for a) **1**, b) **2** and c) **3**. The electron density isosurface is 0.004 a.u.

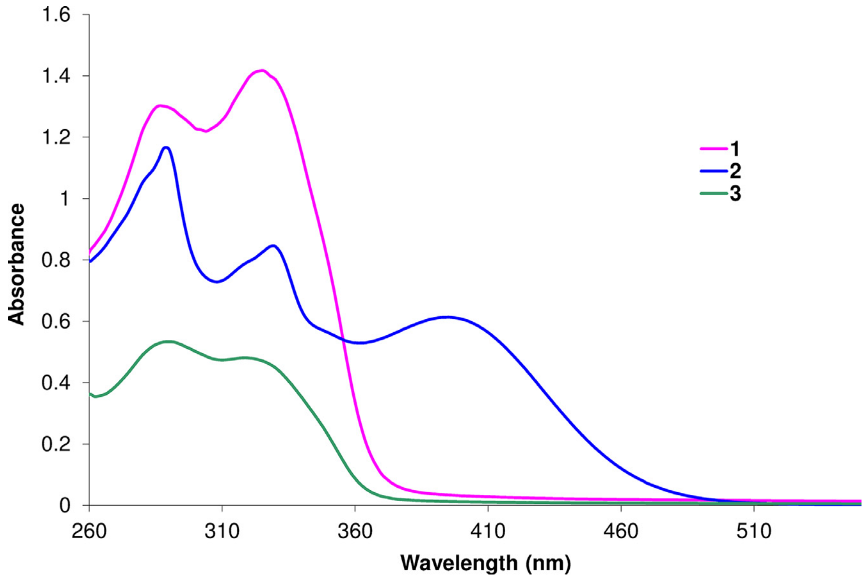

Fig. 5. Electronic absorption spectra of **1–3**, in DMSO.

ing the azido ligands revealing that azido ligand can act as a nucleophile in the catalyst-free [3+2] cycloaddition coupling.

3.5. Electronic structure

The electronic absorption spectra (Fig. 5) of **1–3**, recorded in DMSO, show two main transitions at around 285, and 325 nm corresponding to the medium and low energies π–π^* transitions within the terpyridine residue. In addition, compound **2** has an additional broad band at 396 nm that may be assigned to charge transfer from the morpholine ring to the terpyridine residue.

The nature of the electronic transitions observed in the spectra of **1–3** was investigated by calculating the first 20 singlet states by B3LYP/LANL2DZ method using TDDFT method and the polarizable continuum solvation model to introduce the solvent effect. The calculated electronic transitions and their assignments are given in Table S8. In 250–550 nm range, the TDDFT spectrum of **1** (Fig. 6) is characterized by two bands as well as a shoulder at 293, 464 and 320 nm due to HOMO−2→LUMO+2/LUMO+3, HOMO→LUMO,

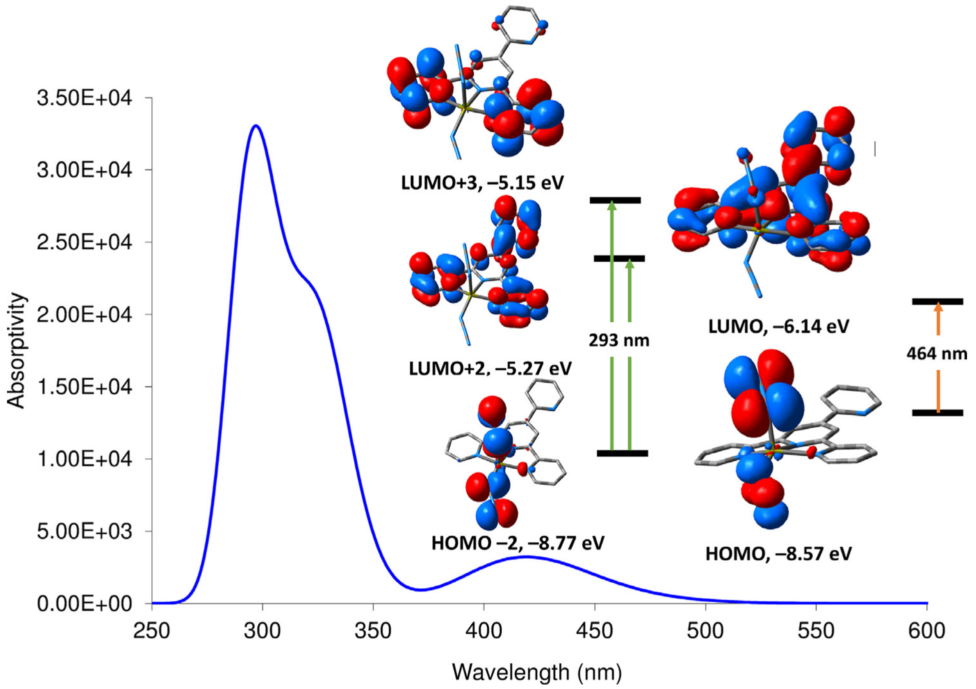

Fig. 6. Computed electronic absorption spectrum of **1** at B3LYP/LANL2DZ and frontier molecular orbitals of some selected transitions.

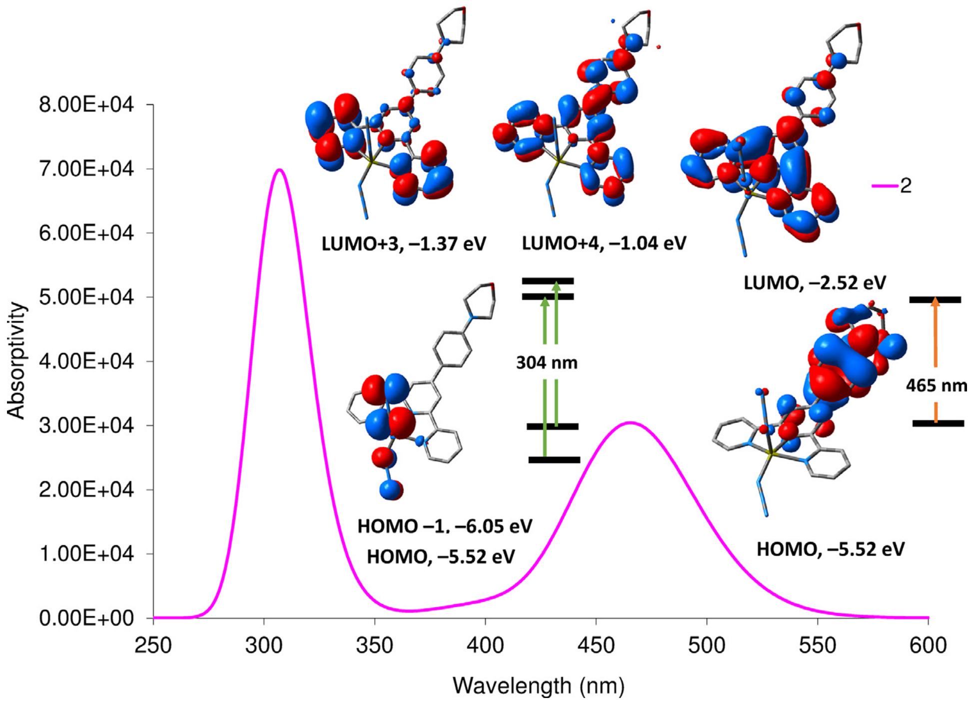

Fig. 7. Computed electronic absorption spectrum of **2** at B3LYP/LANL2DZ and frontier molecular orbitals of some selected transitions.

and HOMO–6→LUMO, respectively. As shown in Fig. 6, the transitions at 293 and 464 nm are LLCT in nature initiating from the azide groups and terminating at the terpy residue. Compound **2** has a similar electronic absorption spectrum to **1**, but the descriptions of frontier molecular orbitals participating in the lowest energy transition and consequently the nature of the transition are different. As shown in Fig. 7, the lowest energy transition at 465 nm (HOMO→LUMO) is assigned to LLCT from morpholine moiety to terpy ligand framework. Like **1**, the band at 304 nm in the spectrum of **2** is LLCT from the azido ligands to terpy residue. The TDDFT spectrum of **3** (Fig. 8) shows one broad band at 411 nm corresponding to HOMO–1→LUMO+3/HOMO→LUMO+2 (37%). Compound **3** is characterized also by two weak electronic transitions at 457 and 426 nm due to HOMO→ LUMO/HOMO–1→LUMO+1 and HOMO–2→LUMO, respectively. As shown in Fig. 8, both HOMO and HOMO–1 orbitals are contained upon the azido ligand, while LUMO+2 and LUMO+3 orbitals are composed of π^* orbitals of terpyridine rings. Thus, the transition at 411 nm is LLCT from the azido ligands to terpyridine framework.

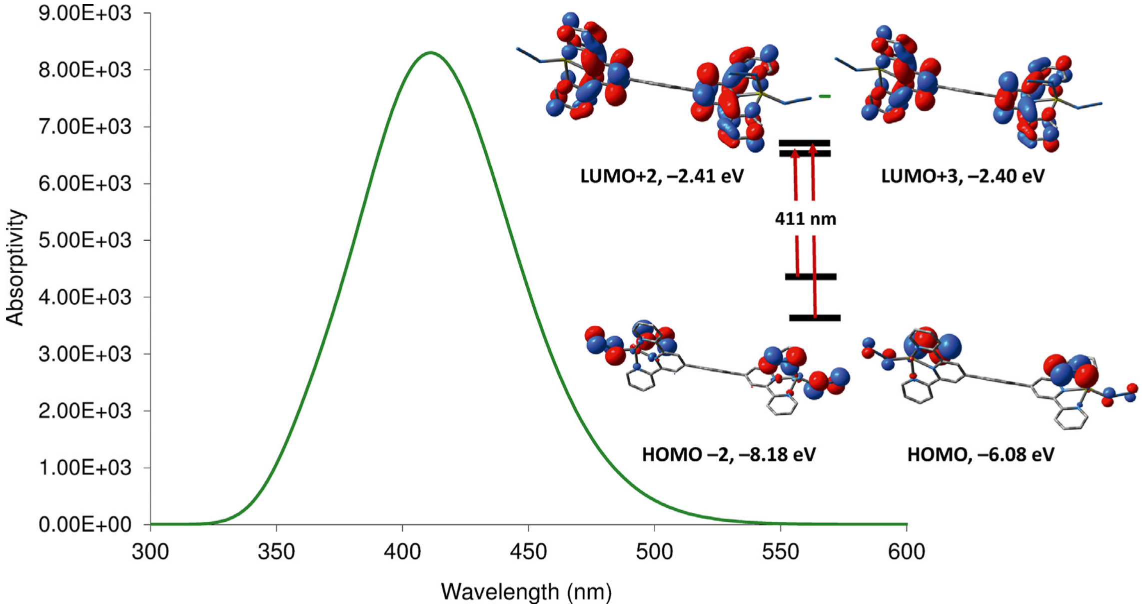

Fig. 8. Computed electronic absorption spectrum of **3** at B3LYP/LANL2DZ and frontier molecular orbitals of some selected transitions.

Conclusion

Owing to the well-known biological applications of Zn(II) complexes and the interest to modify some biomolecules with biologically active compounds *via* the catalyst-free [3+2] cycloaddition coupling, our research group became concerned with the synthesis and characterization of azido Zn(II) complexes to further coupling with electron-poor alkynes. Mono-, and binuclear azido Zn(II) complexes functionalized with tridentate terpyridine derivatives were reported. The spectroscopic, and analytical data as well as the results of density functional theory calculations confirmed that the geometry of the complexes is perfect square pyramidal. The obtained geometries were characterized as local minima owing to the absence of the imaginary vibrational modes. Based on the natural bond orbital analyses, the populations of the 3d-orbitals of the metal centre are corresponding to the oxidation state of Zn(I), not Zn(II), in agreement with the ligand to metal charge transfer. Time dependent density functional theory calculations revealed that the main electronic transitions are LLCT from the azido ligands to the terpyridine residue. Molecular electrostatic potential energy maps showed that the electron rich areas contained upon the azide groups and consequently the azido ligand may act as a nucleophile in the catalyst-free [3+2] cycloaddition coupling.

Data availability statement

The data that support the findings of this study are available in the supplementary material of this article.

Credit Author Statement

Single author publication.

Declaration of Competing Interest

There are no conflicts to declare.

Acknowledgments

A. Mansour thanks the *Alexander von Humboldt* Foundation for Georg Forster postdoctoral fellowship for supporting the stay of the author in Germany and funding of this work. A. Mansour thanks Julius-Maximilians-Universität Würzburg, Germany for giving the author the access to instrumentation to complete and integrate this work. Dr Ola Shehab (Cairo University Faculty of Science, Chemistry Department) is acknowledged for mass spectrometry measurements.

Supplementary materials

Supplementary material associated with this article can be found, in the online version, at doi:10.1016/j.molstruc.2021.130737.

References

[1] a) M.T. Rubino, M. Agamennone, C. Campestre, G. Fracchiolla, et al., Synthesis, SAR, and Biological Evaluation of α-Sulfonylphosphonic Acids as Selective Matrix Metalloproteinase Inhibitors, ChemMedChem 4 (2009) 352–362; b) C.A. Kontogiorgis, P. Papaioannou, D.J. Hadjipavlou-Litina, Matrix metalloproteinase inhibitors: a review on pharmacophore mapping and (Q) SARs results, Curr. Med. Chem. 12 (2005) 339–355; c) Y.-H. Chiu, G.J. Gabriel, J.W. Canary, Ternary Ligand– Zinc– Hydroxamate Complexes, Inorg. Chem. 44 (2005) 40–44; d) A. Scozzafava, C.J. Supuran, Carbonic Anhydrase and Matrix Metalloproteinase Inhibitors: Sulfonylated Amino Acid Hydroxamates with MMP Inhibitory Properties Act as Efficient Inhibitors of CA Isozymes I, II, and IV, and N-Hydroxysulfonamides Inhibit Both These Zinc Enzymes, J. Med. Chem. 43 (2000) 3677–3687.

[2] a) G.H. Eom, H.M. Park, M.Y. Hyun, S.P. Jang, C. Kim, J.H. Lee, S.J. Lee, S.-J. Kim, Y. Kim, Anion effects on the crystal structures of Zn^{II} complexes containing 2,2′-bipyridine: Their photoluminescence and catalytic activities, Polyhedron 30 (2011) 1555–1564; b) S. Olsson, A. Lennartson, M. Håkansson, Absolute asymmetric synthesis of enantiopure organozinc reagents, followed by highly enantioselective chlorination, Chem. Eur. J. 19 (2013) 12415–12423.

[3] a) A. Winter, C. Friebe, M. Chiper, U.S. Schubert, M. Presselt, B. Dietzek, M. Schmitt, J. Popp, Synthesis, Characterization, and Electro-Optical Properties of Zn^{II} Complexes with π-Conjugated Terpyridine Ligands, ChemPhysChem 10 (2009) 787–798; b) S. Chakraborty, D.D. Purkayastha, G. Das, C.R. Bhattacharjee, P. Mondal, S.K. Prasad, D.S.S. Rao, Photoluminescent tetrahedral d^{10}-metal Schiff base complexes exhibiting highly ordered mesomorphism, Polyhedron 105 (2016) 150–158.

[4] S. Mirabella, I.P. Oliveri, F. Ruffino, G. Maccarrone, S. Di Bella, Low-cost chemiresistive sensor for volatile amines based on a 2D network of a zinc (II) Schiff-base complex, Appl. Phys. Lett. 109 (2016) 143108–143122.

[5] Z. Zhu, S. Wang, D. Wei, C. Yang, *Biosens.* Zn^{2+}-cyclen-based complex enable a selective detection of single-stranded thymine-rich DNA in aqueous buffer, Bioelectron 85 (2016) 792–797.

[6] J. Tan, R. Li, D. Li, Q. Zhang, S. Li, H. Zhou, J. Yang, J. Wu, Y. Tian, Thiophene-based terpyridine and its zinc halide complexes: third-order nonlinear optical properties in the near-infrared region, Dalton Trans 44 (2015) 1473–1482.

[7] S.K. Gupta, J. Choudhury, A remote coordination booster enhances the catalytic efficiency by accelerating the generation of an active catalyst, Chem. Commun. 52 (2016) 3384–3387.

[8] P. Sinha, A.K. Sonkar, K. Tripathi, N. Kumari, L. Mishra, Metalloreceptors of the type LML [L=(4′-(2-pyridyl)-2, 2′: 6′, 2 ″-terpyridine), M= Co (II), Cu (II), Zn (II)] for the recognition of Fe^{2+} ions, Polyhedron 134 (2017) 192–198.

[9] W. Fang, C. Liu, Z. Lu, Z. Sun, T. Tu, Tunable reversible metallo-hydrogels: a new platform for visual discrimination of biothiols, Chem. Commun. 50 (2014) 10118–10121.

[10] N. Elgrishi, S. Griveau, M.B. Chambers, F. Bedioui, M. Fontecave, Versatile functionalization of carbon electrodes with a polypyridine ligand: metallation and electrocatalytic H$^+$ and CO$_2$ reduction, Chem. Commun. 51 (2015) 2995–2998.

[11] T. Tsukamoto, R. Aoki, R. Sakamoto, R. Toyoda, M. Shimada, Y. Hattori, M. Asaoka, Y. Kitagawa, E. Nishibori, M. Nakano, H. Nishihara, A simple zinc (II) complex that features multi-functional luminochromism induced by reversible ligand dissociation, Chem. Commun. 53 (2017) 3657–3660.

[12] Z. Ma, Y. Cao, Q. Li, M.F.C. Guedes da Silva, J.J.R. Fraústo da Silva, A.J.L. Pombeiro, Synthesis, characterization, solid-state photo-luminescence and anti-tumor activity of zinc (II) 4′-phenyl-terpyridine compounds, J. Inorg. Biochem. 104 (2010) 704–711.

[13] a) J.E. Moses, A.D. Moorhouse, The growing applications of click chemistry, Chem. Soc. Rev. 36 (2007) 1249; b) P. Thirumurugan, D. Matosiuk, K. Jozwiak, Click chemistry for drug development and diverse chemical–biology applications, Chem. Rev. 113 (2013) 4905–4979.

[14] R. Huisgen, G. Szeimies, L. Mobius, 1.3-Dipolare Cycloadditionen, XXXII. Kinetik der Additionen organischer Azide an CC-Mehrfachbindungen, Chem Ber 100 (1967) 2494–2507.

[15] V.V. Rostpvtsev, L.G. Green, V.V. Fokin, K.B. Sharpless, A stepwise huisgen cycloaddition process: copper(I)-catalyzed regioselective "ligation" of azides and terminal alkynes, Angew Chem Int Ed 41 (2002) 2596–2599.

[16] L.K. Rasmussen, B.C. Boren, V.V. Fokin, Ruthenium-catalyzed cycloaddition of aryl azides and alkynes, Org. Lett. 9 (2007) 5337–5339.

[17] a) H.W. Frühauf, Organotransition metal [3 + 2] cycloaddition reactions, Coord. Chem. Rev. 230 (2002) 79–96; b) W.P. Fehlhammer, W. Beck, Azide chemistry-An inorganic perspective, Part II. [3 + 2]-Cycloaddition reactions of metal azides and related systems, Z. Anorg. Allg. Chem. 641 (10) (2015) 1599–1678.

[18] T.J. Del Castillo, S. Sarkar, K.A. Abboud, A.S. Veige, 1,3-Dipolar cycloaddition between a metal-azide (PPh$_3$PAuN$_3$) and a metal acetylide (Ph$_3$PAuCCPh): An inorganic version of a click reaction, Dalton Trans 40 (2011) 8140–8144.

[19] F. Liu, Y. Lin, P. Yang, [3+ 2] Cycloadditions of molybdenum(II) azide complexes with nitriles and an alkyne, Organometallics 29 (2010) 4282–4290.

[20] A.M. Mansour, K. Radacki, Spectroscopic and antimicrobial activity of photoactivatable tricarbonyl Mn(I) terpyridine compounds, Inorg. Chim. Acta 511 (2020) 119806.

[21] A.M. Mansour, Green-Light-Induced PhotoCORM: Lysozyme Binding Affinity towards Mn^I and Re^I Carbonyl Complexes and Biological Activity Evaluation, Eur. J. Inorg. Chem. (2018) 4805–4811.

[22] A.M. Mansour, O.R. Shehab, K. Radacki, Role of Sulfonate Appendage in the Protein Binding Affinity of Half-Sandwich Ruthenium(II)(η6-p-Cym) Complexes, Eur. J. Inorg. Chem. (2020) 299–307.

[23] A.M. Mansour, O.R. Shehab, K. Radacki, Role of the ancillary ligand in controlling the lysozyme affinity and electronic properties of terpyridine *fac*-Re(CO)$_3$ complexes, Dalton Trans 50 (2021) 1197–1201.

[24] A.M. Mansour, O.R. Shehab, {Ru(CO)$_x$}-core terpyridine complexes: Lysozyme binding affinity, DNA and photoinduced carbon monoxide releasing properties, J. Photochem. Photobiol. A Chem. 364 (2018) 406–414.

[25] M.J. Frisch, G.W. Trucks, H.B. Schlegel, G.E. Scuseria, M.A. Robb, J.R. Cheeseman, V.G. Zakrzewski, J.A. Montgomery, R.E. Stratmann, J.C. Burant, S. Dapprich, J.M. Millam, A.D. Daniels, K.N. Kudin, M.C. Strain, O. Farkas, J. Tomasi, V. Barone, M. Cossi, R. Cammi, B. Mennucci, C. Pomelli, C. Adamo, S. Clifford, J. Ochterski, G.A. Petersson, P.Y. Ayala, Q. Cui, K. Morokuma, D.K. Malick, A.D. Rabuck, K. Raghavachari, J.B. Foresman, J. Cioslowski, J.V. Ortiz, A.G. Baboul, B.B. Stefanov, G. Liu, A. Liashenko, P. Piskorz, I. Komaromi, R. Gomperts, R.L. Martin, D.J. Fox, T. Keith, M.A. Al-Laham, C.Y. Peng, A. Nanayakkara, C. Gonzalez, M. Challacombe, P.M.W. Gill, B.G. Johnson, W. Chen, M.W. Wong, J.L. Andres, M. Head-Gordon, E.S. Replogle, J.A. Pople, GAUSSIAN 03 (Revision A.9), Gaussian, Inc., Pittsburgh, 2003.

[26] A. Frisch, A.B. Nielson, A.J. Holder, Gaussview User Manual, Gaussian, Inc, Pittsburgh, PA, 2000.

[27] L. Gou, Crystal structure of (4′-(2-pyridyl)-2, 2′: 6′, 2" terpyridine) zink(II) diazide, Zn (C$_{20}$H$_{14}$N$_4$)(N$_3$)$_2$, Z. Kristallogr 224 (2009) 561–562.

[28] A.D. Becke, Density-functional thermochemistry. III. The role of exact exchange, J. Chem. Phys. 98 (1993) 5648–5652.

[29] a) P.J. Hay, W.R. Wadt, Ab initio effective core potentials for molecular calculations. Potentials for the transition metal atoms Sc to Hg, J. Chem. Phys. 82 (1985) 270–283; b) P.J. Hay, W.R. Wadt, Ab initio effective core potentials for molecular calculations. Potentials for main group elements Na to Bi, J. Chem. Phys. 82 (1985) 284–298.

[30] T. Yanai, D.P. Tew, N.C. Handy, A New Hybrid Exchange-Correlation Functional Using the Coulomb-Attenuating Method (CAM-B3LYP), Chem. Phys. Lett. 393 (2004) 51–57.

[31] Y. Zhao, N.E. Schultz, D.G. Truhlar, Exchange-correlation functional with broad accuracy for metallic and nonmetallic compounds, kinetics, and noncovalent interactions, J. Chem. Phys. 123 (2005) 161103–161107.

[32] A.W. Addison, T.N. Rao, J. Reedijk, J.V. Rijn, G.C. Verschoor, Synthesis, structure, and spectroscopic properties of copper(II) compounds containing nitrogen–sulphur donor ligands; the crystal and molecular structure of aqua[1,7-*bis*(N-methylbenzimidazol-2′-yl)-2,6-dithiaheptane]copper(II) perchlorate, J. Chem. Soc. Dalton Trans. (1984) 1349–1356.

[33] a) G. Rauhut, P. Pulay, Transferable scaling factors for density functional derived vibrational force fields, J. Phys. Chem. 99 (1995) 3093–3100.

[34] A.E. Reed, L.A. Curtiuss, F. Weinhold, Intermolecular interactions from a natural bond orbital, donor-acceptor viewpoint, Chem. Rev. 88 (1988) 899–926.

[35] A.M. Mansour, Selective coordination ability of sulfamethazine Schiff-base ligand towards copper (II): Molecular structures, spectral and SAR study, Spectrochim. Acta part A 123 (2014) 257–266.